Analyst

MINIREVIEW

View Article Online
View Journal | View Issue

Cite this: *Analyst*, 2018, **143**, 2448

Recent advances in merging photonic crystals and plasmonics for bioanalytical applications

Bing Liu, [a,b] Hosein Monshat,[c] Zhongze Gu, *[a,b] Meng Lu*[c,d] and Xiangwei Zhao *[a,b]

Photonic crystals (PhCs) and plasmonic nanostructures offer the unprecedented capability to control the interaction of light and biomolecules at the nanoscale. Based on PhC and plasmonic phenomena, a variety of analytical techniques have been demonstrated and successfully implemented in many fields, such as biological sciences, clinical diagnosis, drug discovery, and environmental monitoring. During the past decades, PhC and plasmonic technologies have progressed in parallel with their pros and cons. The merging of photonic crystals with plasmonics will significantly improve biosensor performances and enlarge the linear detection range of analytical targets. Here, we review the state-of-the-art biosensors that combine PhC and plasmonic nanomaterials for quantitative analysis. The optical mechanisms of PhCs, plasmonic crystals, and metal nanoparticles (NPs) are presented, along with their integration and potential applications. By explaining the optical coupling of photonic crystals and plasmonics, the review manifests how PhC–plasmonic hybrid biosensors can achieve the advantages, including high sensitivity, low cost, and short assay time as well. The review also discusses the challenges and future opportunities in this fascinating field.

Received 24th January 2018,
Accepted 15th April 2018

DOI: 10.1039/c8an00144h

rsc.li/analyst

[a]*State Key Laboratory of Bioelectronics, School of Biological Science and Medical Engineering, Southeast University, Nanjing 210096, China. E-mail: xwzhao@seu.edu.cn, gu@seu.edu.cn*
[b]*National Demonstration Center for Experimental Biomedical Engineering Education, Southeast University, Nanjing 210096, China*
[c]*Department of Mechanical Engineering, Iowa State University, Ames, Iowa 50011, USA. E-mail: menglu@iastate.edu*
[d]*Department of Electrical and Computer Engineering, Iowa State University, Ames, Iowa 50011, USA*

Introduction

Photonic crystals (PhCs) and plasmonic nanostructures are capable of manipulating the interaction of light and biomolecules at the microscale and nanoscale, which are widely used in biosensors.[1–6] In particular, optical resonances supported by nanophotonic devices have been harnessed to facilitate the analysis of biomaterials, such as small compounds,

Bing Liu

Bing Liu received his Ph.D. degree in Biomedical Engineering from Southeast University in 2018. He is working as a postdoctoral researcher at the School of Biological Science and Medical Engineering, State Key Laboratory of Bioelectronics, Southeast University, in the group of Professor Xiangwei Zhao. His research interests focus on the development of multiplex bioassays based on photonic crystals and SERS nanotags.

Hosein Monshat

Hosein Monshat received his M.S. from Iowa State University, United States, in 2016. Currently he is a Ph.D. candidate at Iowa State University at the Mechanical Engineering Department working under the supervision of Dr Meng Lu. His research interests include photonics, plasmonics, infrared optics, and the interactions between near-field light and heat energies. Currently, he is the treasurer of Optical Society of America (OSA) Student Chapter at Iowa State University.

DNAs, proteins, and cells.[7–9] This new category of analytical methods offers many advantages, including high sensitivity, low cost, and short assay time as well. In the past two decades, photonic crystals and plasmonic nanostructures have been developed in parallel, and both materials have been successfully implemented in many analytical methods depending on their unique optical characteristics. On the other hand, the combination of these two types of nanophotonic technologies can integrate multiple detection mechanisms into a single device with enhanced performances. The hybrid sensors can take advantage of the collective PhC–plasmonic resonances of metal and dielectric cavities. Because the coupled PhC–plasmonic resonances can be precisely engineered using the state-of-the-art nanofabrication processes and demonstrated by electromagnetic (EM) simulations, the hybrid sensors would provide unprecedented sensing capability and open the path to novel biosensing applications. As a mini-review, the paper first briefly discusses the features of PhC and plasmonic nanostructures. Then, we present the recent developments in integrating PhCs and plasmonics into a single device and elaborate how to use the coupling of these two optical resonances for bioanalytical applications.

Yablonovitch[10] and John[11] in 1987 demonstrated the first PhC devices which consisted of periodic structures with alternating refractiveindices. Later, PhCs were exploited to guide, localize, and manipulate light on a sub-wavelength scale. Cunningham *et al.* first reported label-free detection with PhCs.[12–17] There are two major categories of PhCs, including PhC slabs[18,19] and three-dimensional (3D) photonic crystals of dielectric materials.[20,21] The PhC slabs refer to the dielectric waveguide with one-dimensional (1D) and two-dimensional (2D) periodic modulations of the material refractive index along the surface.[22] The PhC slab may carry linear or 2D gratings, such as arrays of holes or posts arranged in a rectangular or hexagonal grid, which have been designed to support different types of optical resonances, such as the leaky mode resonance and the in-plane cavity mode when a defect is introduced into the periodic gratings. Until now, the optical resonances of the PhC slabs have been used for label-free and fluorescent assays to facilitate the detection of chemicals and biomolecules.[12–14,23]

3D PhC structures, being analogous to semiconductor crystals, can exhibit full photonic band gaps (PBGs) in a specific range of wavelength. Within the PBGs, the lack of mode prohibits the progagation of light, and thus the 3D PhCs show strong reflection. For PhCs with PBGs in the visible or near-infrared wavelength ranges, their periods are on the scales of several hundred nanometers. Owing to the complicated 3D structure, the fabrication of microscale and nanoscale PhC structures is challenging. Fortunately, various 3D PhCs existing in nature render striking colors. For example, the PhCs of *Morpho* butterflies, *Paracaudina chilensis*, some beetles, and opals display structural colors at the PBG.[24–26] The period of PhCs determines the spectral position of the PBGs and the structural color. As a response to stimulus, the PhC's period may change and consequently shift the color displayed by the PhC. Based on this principle, many analytical approaches have been developed to quantify physical,[27–31] chemical,[32–35] or biological[36] stimuli. It is particularly important that the PhCs have been deployed as a label-free biosensor to detect target biomolecules by measuring the change of the refractive index. The distinct colors of different PhCs can be applied to achieve a high throughput, multiplex and label-free assay.[37–39] Despite its success in analytical applications, the PhC-based sensors still have some shortcomings. For example, the 3D PhC struc-

Zhongze Gu

Zhongze Gu has been a Professor of Cheung Kong Scholars of Biomedical Science and Medical Engineering, Southeast University, since 2003. He obtained his M.S. and Ph.D. degrees from Southeast University and University of Tokyo in 1992 and 1998, respectively. Later, he had been working as a researcher at the Kanagawa Academy of Science and Technology. He then began a project to study opal photonic crystals and did a lot of excellent work in this field. Now he is the dean of School of Biological Science and Medical Engineering, the director of State Key Laboratory of Bioelectronics. His research studies are related to bio-inspired intelligent materials, photonic crystal, biosensors and bioelectronics. He has published more than two-hundred research papers in international journals and applied for more than 70 related patents.

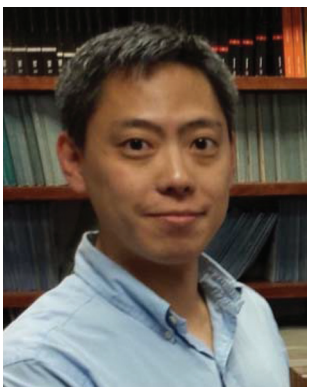

Meng Lu

Meng Lu received M.S. and Ph.D. degrees in electrical and computer engineering from the University of Illinois at Urbana–Champaign, Urban, in 2004 and 2008, respectively. He is currently an Assistant Professor in the Department of Electrical and Computer Engineering and Department of Mechanical Engineering at the Iowa State University. His group focuses on nanophotonics for energy and biomedical applications. His prior appointments include being a research scientist at SRU Biosystems at Woburn, MA and the Adjunct Assistant Professor in the Electrical and Computer Engineering Department, the University of Illinois at Urbana-Champaign from 2009 to 2013.

tures can display a color change owing to the attachment of biomolecules but the local electromagnetic field of the 3D PhC is too weak to be adopted for fluorescent- or Raman-based assays.[40] On the other hand, it is possible to achieve a high *Q*-factor (high *Q*) optical resonance with a significantly enhanced near-field using PhC slabs. The high-*Q* PhC slab, which can achieve the enhancement factor greater than three orders of magnitude, has been used to facilitate fluorescence and Raman detection.[41–44] However, the coupling of light into high *Q* modes requires stringent control of coupling conditions. These problems can be effectively addressed by introducing plasmonics into PhC structures.

Plasmonic materials, such as metal thin film with periodic patterns and noble metal nanoparticles (NPs), can interact strongly with light through plasmonic resonance. Plasmonic structures have been extensively studied for analytical applications. For example, surface plasmon polariton (SPP) modes can be utilized to develop refractometric biosensors because of their high sensitivity to the change of the surrounding refractive index.[45,46] The localized surface plasmon resonance (LSPR) modes supported by metal nanostructures have been exploited for surface enhanced Raman scattering (SERS) and metal-enhanced fluorescence.[47–52] Compared to PhCs, plasmonics-based nanosensors can be much smaller than the wavelength and offer significantly enhanced near-fields. Plasmonic materials can either be incorporated with PhCs, or can even be fabricated as periodic structures to form metal PhCs, *i.e.*, plasmonic crystals.[53–55] Both approaches can be used to miniaturize the dimension of sensors and improve analytical performances. In recent years, plasmonic crystals prepared by the microfabrication method have attracted enormous attention due to their characteristics of the highly ordered structure, tunable period, and controllable "hot spots" which are associated with the enhanced near-field. For example, Macias *et al.* have reported plasmonic crystals fabricated with soft nanoimprint lithography and simulated the distribution of their electric field intensity.[56] The enhancement factor was calculated which exceeded 10^7 in the case of benzenethiol and 10^{10} when 4-mercaptopyridine was used. However, the microfabricated plasmonic crystals have not been widely applied due to the stability and cost of fabrication.

At present, there are sufficient literature studies on PhC- and plasmonic-based biosensors. The minireview focuses on the biosensing technology that takes advantage of the integration of PhCs and plasmonics. Generally, there are two methods to achieve a hybrid device: 1. Attaching metal nanoparticles to PhC backbones, where the metal nanoparticles can be *in situ* synthesized or conjugated to the PhCs; and 2. Using a thin metal film as the cladding layer of the PhCs to support both plasmonic and PhC resonances. Both of these methods can be adopted depending on the specific application. It is worth noting that the design of photonic crystals requires low-loss materials to warrant a strong resonance with a high quality-factor (*Q*-factor), but the introduction of the lossy metals can deteriorate the *Q*-factor. On the other hand, the reduced *Q*-factor implicates a less stringent condition to couple the resonance with optical excitations. The tradeoff between the metal-induced loss and the plasmon-enhanced EM field needs to be balanced at the design stage of the hybrid sensors. The rest of the minireview consists of two sections that illustrate three different directions to explore the collective phenomena in PhCs and plasmonic nanostructures. Following the reviews of recent progress, we present an outlook for the future development.

Plasmon integrated photonic crystal slab surface

Owing to the excitation without the need of a special coupling mechanism, the leaky mode resonance has been focused on the plasmon-enhanced 1D and 2D photonic crystal surfaces. The leaky mode resonance, also known as the guided-mode resonance (GMR), exhibits narrowband optical resonance under broadband light illumination. The GMR effect was first discovered by Hessel and Oliner in 1965[57] and later named by Magnusson *et al.* in the early 1990s.[58–60] The GMR mode exists because part of the excitation is coupled into the waveguide at resonance, while the rest is either reflected or transmitted. When the light coupled into the PhC slab leaks outwards, constructive interference between the out-coupled and reflected light yields a sharp resonant reflection peak with the efficiency of nearly 100%. In contrast, the transmission shows a sharp resonant dip with almost 0% efficiency due to the destructive interference between the out-coupled and the transmitted light. For a specific combination of incident angle and wavelength, phase matching by the grating allows the incident beam to be coupled into the desired GMR mode.[61,62] The unique feature of the GMR-based PhC slabs have been successfully implemented in refractive index-based biosensors.[12] It is particularly interesting that when the excitation light is coupled to the GMR resonance, the EM field intensity in the close vicinity of the slab surface becomes strongly enhanced compared to the intensity of the excitation. This phenomenon has been deployed to enhance the sensitivity of fluorescence-

Xiangwei Zhao

Xiangwei Zhao received his Ph.D. degree in 2006 from Zhejiang University and then joined Southeast University. Currently, he is a professor at the State Key Laboratory of Bioelectronics, School of Biological Science and Medical Engineering, Southeast University. His research interests lie in nanophotonics, single cell analysis and biomedical big data.

based assays, such as DNA and protein microarrays.[63–66] Recently, the same principle can also be applied to excite surface plasmons with an extraordinarily strong local EM field.

The characteristics of the PhC slab, such as its resonance wavelength, peak reflection efficiency, and linewidth, are determined by the geometrical and material properties of the device.[67] Since the period of the GMR gratings is smaller than the resonance wavelength, the production of the sub-wavelength grating for the visible and near-infrared wavelength ranges requires a nanoscale fabrication process. Several established processes, such as deep UV lithography, holographic lithography, interference lithography, and nanoimprint lithography, have been successfully adopted for PhC fabrication.[68–71] Among these methods, the nanoimprint lithography approach is capable of manufacturing 1D and 2D PhC slabs with high throughput, sufficient fidelity, and relatively low cost.[72] The inexpensive approach can produce PhCs over continuous rolls of flexible plastic film and enable PhC biosensors to be economically compatible with single-use and disposable applications. On the other hand, plasmonic nanoparticles can be added onto the fabricated PhC slabs by physical vapor deposition or immobilization of NPs. This section reviews some examples to illustrate how the coupling of PhC slabs and plasmonic NPs can be exploited for the detection of chemicals and biomolecules.

The metal nanoparticle can be deposited on the surface of PhC slabs using the glancing angle deposition (GLAD) technology.[43,73] The GLAD method uses a conventional e-beam evaporator with the angle between the surface of the PhC slab and the evaporating flux less than 15° to create metal NPs. Through the GLAD method, Kim *et al.* demonstrated a PhC-enhanced SERS substrate, which consisted of a 1D PhC slab as the dielectric optical resonator, SiO_2 nanorods as the layer spacer, and silver NPs appeared as a cap structure at the top of the substrate (Fig. 1a–c).[74,75] The PhC substrate can effectively couple light to the silver NPs deposited on the PhC surface when the incident light wavelength and the angle are tuned to match the PhC resonant coupling conditions. As shown in Fig. 1d–f, the coupling of the PhC resonance and the plasmonic resonance results in the strikingly strong electromagnetic field at the "hot spots". The Ag NP coated PhC slab was used to detect *trans*-1,2-bis (4-pyridyl) ethane (BPE). In comparison with the SERS performance of an ordinary glass substrate coated with the same SiO_2–Ag nanostructure, an additional SERS enhancement factor of 10–30× was achieved with the PhC substrate (Fig. 1e). In addition, when the resonance angles are ±13°, the simulated $|E|^4$ are maximized, as well as the maximized Raman signal (Fig. 1f). The limit of detection (LOD) for BPE was calculated to be 0.3–3 fM. Later, the group optimized the coupling between the GMR modes of PhC and plasmonic modes of silver NPs to maximize the Raman scattering signal. The results showed an additional enhancement factor of 21.4 when the coupling efficiency was maximized with the SiO_2 layer thickness of 50 nm and the Ag NP size of about 40 nm.[75] Except for the Ag NPs which can be deposited on the PhC slab for Raman enhancement, gold NPs can also be used as enhanced agents because of their special optical properties, simple synthesis, easy size control, and good biocompatibility. For example, recently, Liu *et al.* showed that the coupling of PhC resonance and gold nanorods can produce a greatly amplified local field, which could be used to improve the SERS detection of R6G molecules.[76]

Besides through physical deposition, the metal NPs can be absorbed on the PhC surface *via* biomolecule linkers for detec-

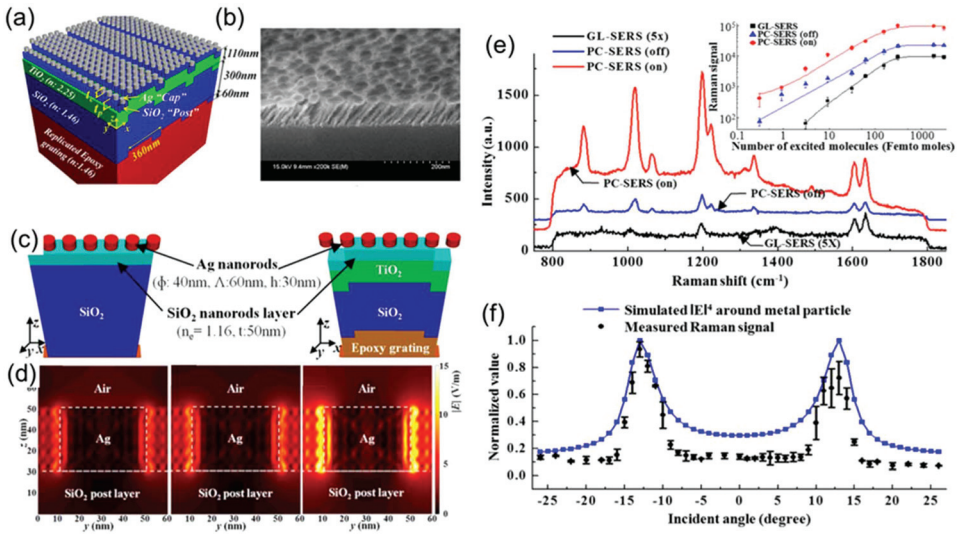

Fig. 1 Ag nanoparticles on a PhC substrate. (a) Schematic diagram of the Ag nanorod-based PhC substrate with a SiO_2 spacer layer. (b) SEM of the Ag nanorods deposited by the GLAD method. (c) Simulation model of the PhC–Ag nanorod hybrid device. (d) Simulated electric-field distribution for a single Ag nanostructure on a flat surface (left panel), the PhC substrate without a resonance (middle panel), and the PhC substrate with the GMR resonance (right panel). (e) Raman spectra of BPE on glass and PhC substrates under on/off resonance conditions. (f) Comparison of the measured Raman signal and simulated $|E|^4$ for varying incident angles. Reproduced with permission from ref. 74 and 75.

tion and imaging. Zhao *et al.* explored the new detection mechanism using the gold NPs on 1D PhCs based on the photothermal and photoacoustic effects.[77,78] Owing to the strong photothermal effect of gold NPs, gold NPs have been adopted as a labeling material for photoacoustic immunoassay.[79,80] The photoacoustic and photothermal detection of NPs can be enhanced by the PhC slab. The results showed that the photoacoustic signal of the gold NPs was enhanced by a factor of 40 by coupling the excitation light into the GMR mode. Based on a pump–probe scheme, the PhC-enhanced photothermal lens technology has been recently demonstrated to improve the detection of gold NPs by 20-fold.[81]

3D photonic crystal incorporated with plasmonic nanoparticles

Plasmonic NPs have been broadly used in LSPR or SERS-based biosensors.[82–87] However, the sensitivity of LSPR-based biosensors depending on the shift of absorption spectra is limited and it is difficult to control the distribution and accessibility of the plasmonic NP "hot spots", which mainly contribute to SERS.[88] This is also the reason for their performance discounts in practical applications. In this case, the merging of plasmonic NPs and 3D PhC can help a lot since its 3D ordered nanostructure could efficiently adjust the distribution and accessibility of "hot spots". In addition, PhC can regulate the local density of states with its bandgap, which could be utilized to improve the interaction between light and plasmonic materials.[40]

The self-assembly of massively synthesized monodisperse nanoparticles is the most commonly used method to fabricate artificial 3D PhCs, which has proved to be cost-efficient and compatible to versatile surfaces, volumes, and processes like printing.[89–91] Due to the interstices between nanoparticles, the resultant colloidal PhC structure is highly porous, beneficiating a high surface to volume ratio (SVR) desired by analysis and providing the advantages of fluidic channels at the nanoscale. For example, Zhao *et al.* reported a gold nanoparticles incorporated inverse opal photonic crystal (IO PhC) capillary (Fig. 2a and b) for the SERS detection of creatinine in artificial samples with a detection limit of 0.9 mg dL^{-1} (Fig. 2c).[92] This nanostructured capillary tube integrated the SERS sensor and the nanofluidic structure to offer delivery and analysis of samples simultaneously. In addition, the *E*-field around nanoparticles in the IO PhC was enhanced remarkably compared with that in the capillary without the PhC structure (Fig. 2d). The "hot spots" in the 3D nanostructure were more uniform and controllable, indicating the modulation of the *E*-field distribution with the PhC. This optofluidic detection device opens a new window for the application of point-of-care testing (POCT). The merging of PhC and plasmonic materials can also be used for the capture and detection of microbes in a similar optofluidic way. Wang *et al.* proposed a silver-plated PhC substrate as a bacterial filter owing to the ordered porosity of the structure in tens of nanometers.[93] The substrate showed strong and uniform distribution of "hot spots" accompanying the nanofluidic channels, which is crucial for SERS measurement. The bacteria could be detected in a "drop and measure" manner with a portable Raman spectrometer (Fig. 3a and b). Electricigens are a kind of microbe that can directly reduce a

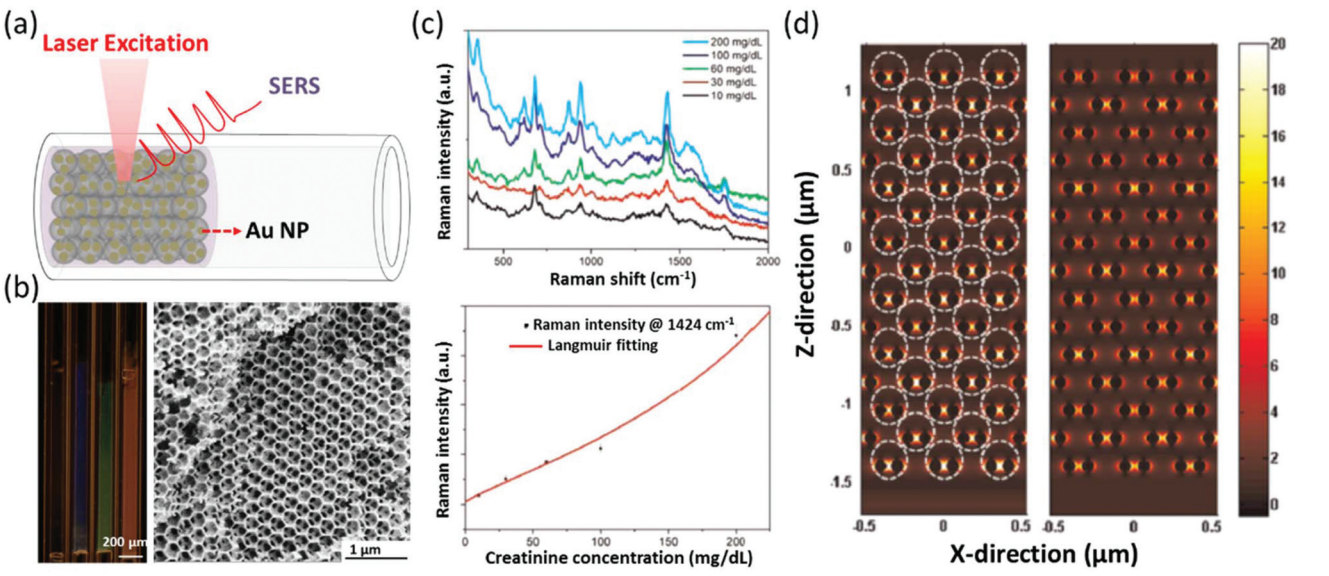

Fig. 2 Structure and analysis performance of the IO PhC capillary. (a) Schematic structure of the gold NP incorporated IO PhC capillary. (b) Optical microscope image of four IO PhC capillaries (left panel); the cross section of the structure inside the capillary (right panel). (c) Raman spectra of creatinine at different concentrations (up panel); the calibration curve of the Raman intensity as a function of the creatinine concentration (down panel). (d) The simulated $|E/E_{inc}|$ profile of the gold NP incorporated IO PhC capillary (left panel) and gold NPs in the capillary (right panel) with a 785 nm laser. Reproduced with permission from ref. 92.

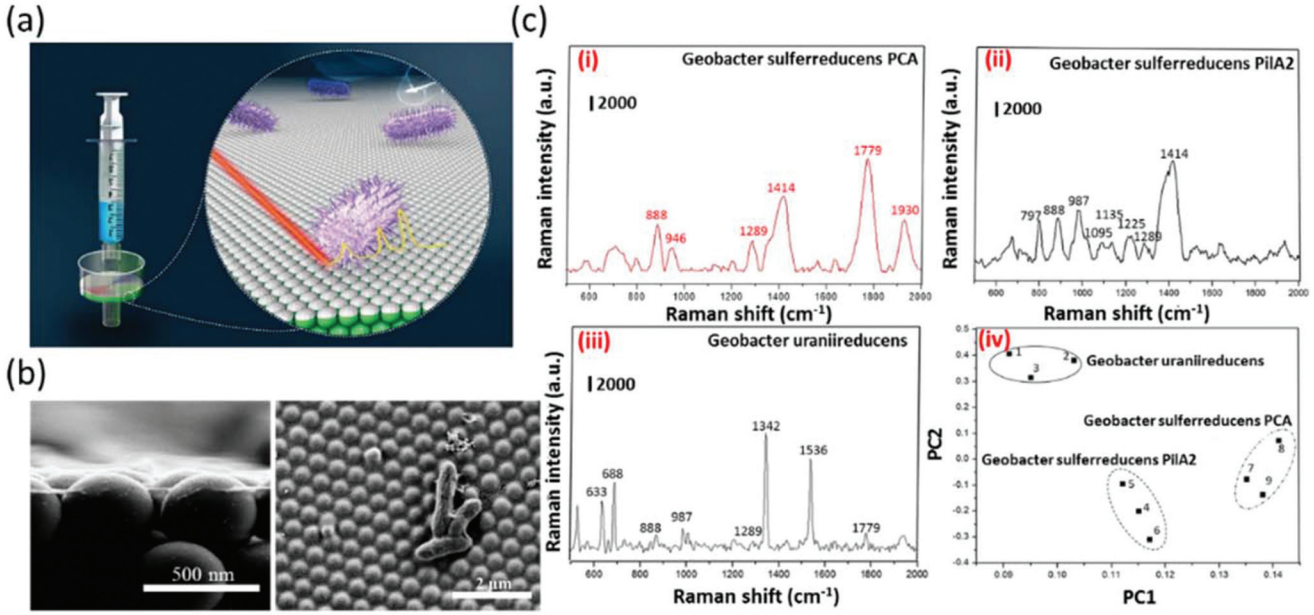

Fig. 3 Scheme and application in electricigens discrimination of the silver-plated PhC filter. (a) Scheme of the silver-plated PhC filter. (b) SEM image of the cross-section of the silver-plated PhC (left panel) and the surface with bacterium on it (right panel). (c) Raman spectra of *Geobacter sulferreducens PCA* (i), *Geobacter sulferreducens PilA 2* (ii), *Geobacter uraniireducens* (iii), and the principal component analysis of these three strains (iv). Reproduced with permission from ref. 93.

metallic anode through the processes of extracellular electron transfer, which allowed one to construct microbial fuel cells (MFCs) for power generation. With this plasmonic filter, they could distinguish electricigens with not only species and strain specificity, but also regarding wild and mutant types (Fig. 3c). With respect to the conventional PCR or the cultiva-

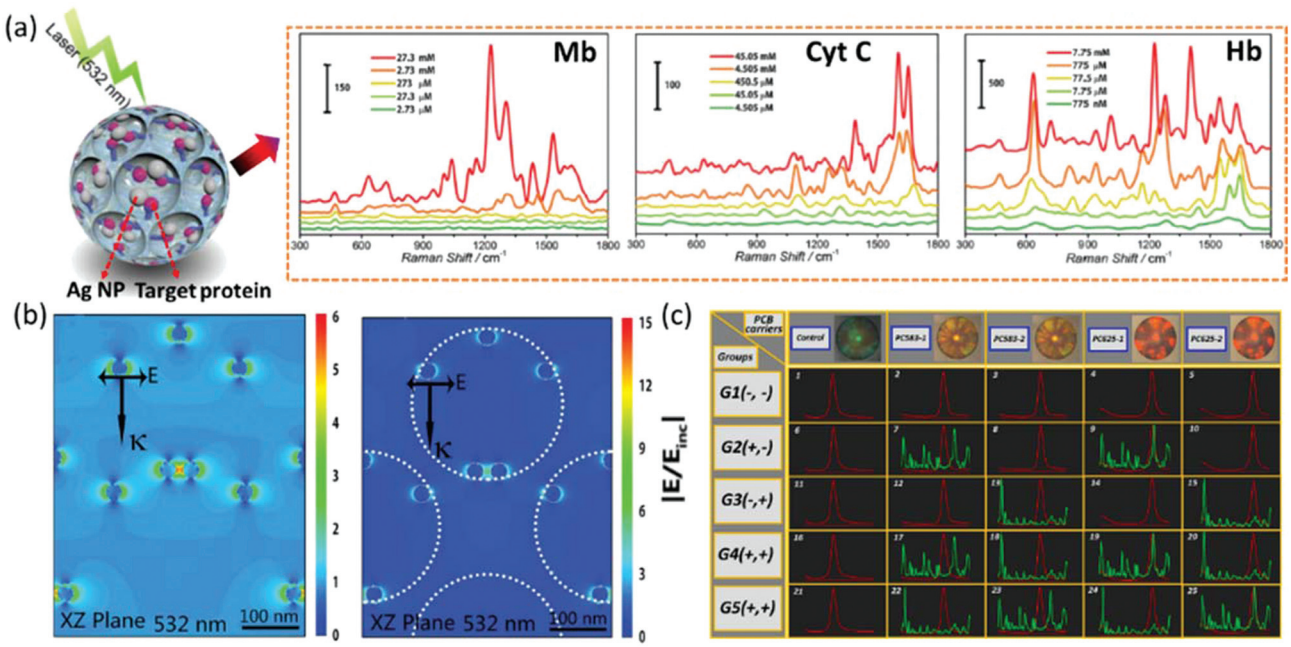

Fig. 4 Scheme and multiplexed analysis results of IOPCBs and PCBs. (a) Scheme diagram of IOPCBs for multiplexed analysis of proteins by their Raman spectra (left panel); Raman spectra of three proteins (mouse myoglobin (Mb), Cyt C, and human hemoglobin (Hb)) with different concentrations (right panel). (b) The simulated $|E/E_{inc}|$ profiles in the Ag NPs (left panel) and the Ag NP hybridized IOPCB (right panel). (c) Multiplex bioassay of qualitative detection of mouse IgG and rabbit IgG by PCBs and SERS nanotags. Reproduced with permission from ref. 40 and 95.

tion method, this method exhibits great potential in the quick screening of microbes in fields of environmental monitoring and disease control as well as cell analysis.

Multiplex biomarker detection is a key issue not only in POCT, but also in high throughput screening in the acquisition of biomedical big data. To identify multiple proteins directly by their SERS spectra, hydrogel inverse opal PhC was used as a support and multiple proteins were captured and stained with silver NPs (Fig. 4a).[40] Due to the high density "hot spots" in the 3D structure and the local electromagnetic field at the bandgap of the inverse opal photonic crystal bead (IOPCB), PhC offered an extra 9 times enhancement compared

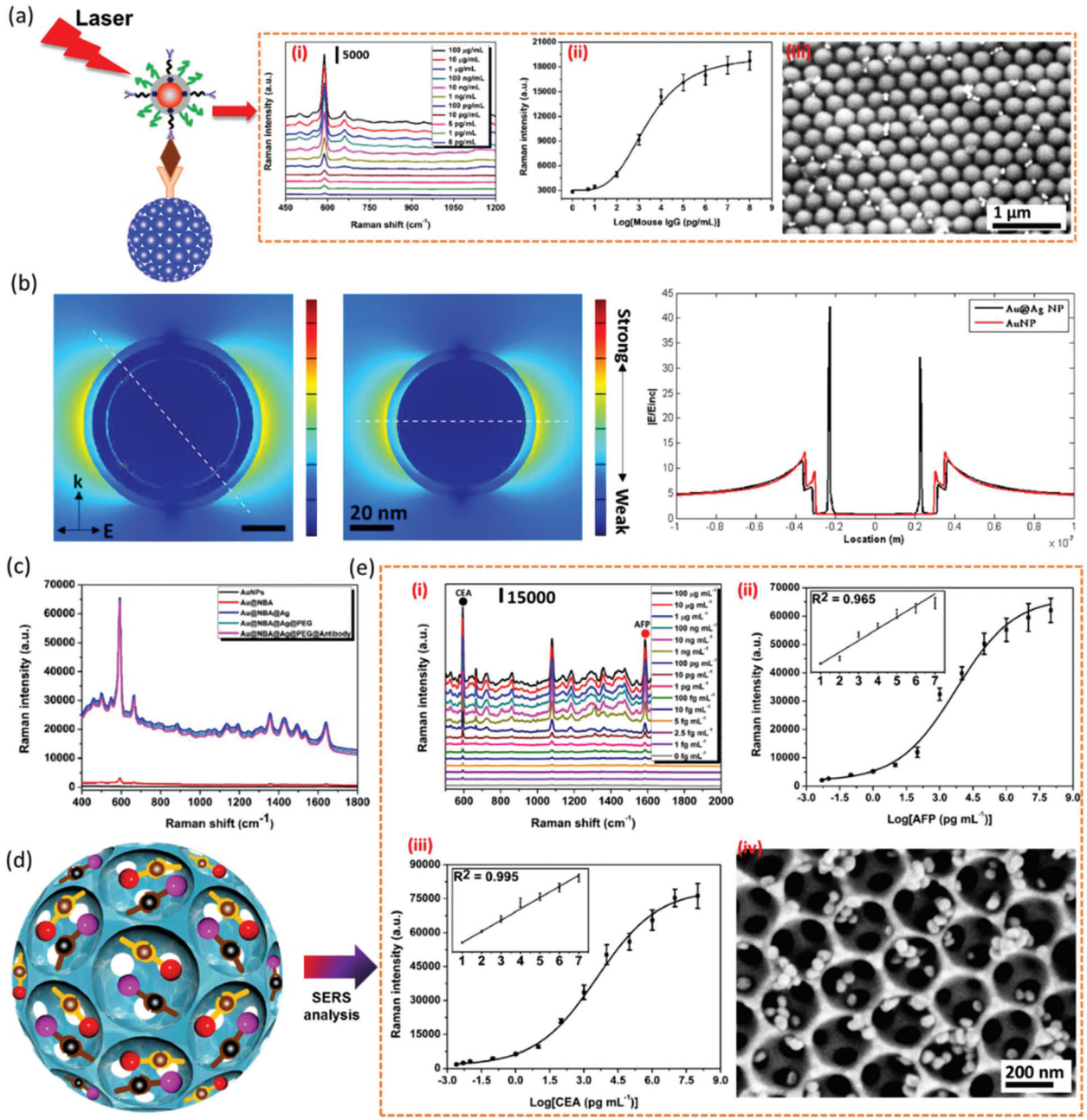

Fig. 5 Multiplex analysis with PCB and Au@Ag NP-based SERS nanotags. (a) Schematic illustration of highly sensitive detection by SERS nanotag and PCB (left panel); (right panel) Raman spectra of different concentrations of mouse IgG (i); reference plot of Raman intensities at Raman shift of 595 cm^{-1} *vs.* logarithm of mouse IgG concentrations (ii); high magnification SEM image of SERS nanotags on the PCB surface after the immunoreaction (iii). (b) The simulated $|E/E_{inc}|$ profiles of Au@Ag NP (left panel) and Au NP (middle panel); comparison of the $|E/E_{inc}|$ profile along the maximum point-line (right panel). (c) Raman spectra of SERS nanotags. (d) Schematic diagram of multiplex protein biomarker detection on a single IOPCB by SERS nanotags. (e) Raman spectra at different concentrations of AFP and CEA (i); dose–response curves of AFP (plotted with Raman intensity at 1585 cm^{-1}, ii) and CEA (plotted with Raman intensity at 595 cm^{-1}, iii), respectively; SEM image of the IOPCB surface after the reaction with SERS nanotags (iv). The inset is the linear part of the reference plot. Reproduced with permission from ref. 97 and 101.

with the Ag NPs without the PhC structure (Fig. 4b). Hence the intensity of the Raman signal of proteins was improved remarkably and multiple proteins were label-free detected by their SERS spectra. However, larger capacity of multiplicity is needed for precision medicine or biomedical big data. The label-free identification of tens or hundreds of proteins by their fingerprints of Raman or SERS spectra is complex. Recently, SERS encoded nanotags have shown great promise in molecule analysis with high encoding capacity and ultrahigh sensitivity down to a single molecule.[87] But SERS encoding capacity is also limited because of the limited number of available Raman dyes with robust and precise readouts.[5] PhCs are widely used as an encoded carriers for multiplex bioassays due to their PBGs although the encoding capacity is also limited.[94] Therefore, by combining carriers of PhC and nanotags of SERS, the encoding capacity of multiplex detection will be easily increased to the product of their encode number (Fig. 4c).[95] Furthermore, unlike fluorescence dyes or quantum dots, SERS nanotags could be easily washed out from the PCB surface because of their larger size, which leads to a high signal to noise ratio (SNR) desired for highly sensitive and quantitative analysis.

In quantitative multiplex detection, the concentrations of multiple analytes usually differed in the range from pg mL^{-1} to sub mg mL^{-1}. Hence the linear dynamic range (LDR) is a critical point needing to be considered. With a wide LDR, sample dilutions or concentrations will be avoided or reduced before they are analyzed.[96] Therefore, in practice of multiplex assays, the method with both high sensitivity and a wide LDR is in great need with respect to the simplification of sample pretreatments and cost effectiveness. Gold–silver core–shell (Au@Ag) NPs can further increase the signal intensity of SERS nanotags (Fig. 5a).[97] When the silver shell grows on the surface of the gold core, plasmon coupling effects between the core and the shell become significant because of the stronger interaction between them.[98–100] The hybridization of the plasmons of the bimetal results in larger splitting of bonding and anti-bonding modes, leading to the excitation of the higher order modes, and thus the *E*-field intensity of the interior gap region of the Au@Ag NP is 4.55 times that of the Au NP (Fig. 5b) and the Raman intensity increased by 19 times as measured (Fig. 5c). The LOD is improved by 14 times correspondingly. On the other hand, owing to the higher SVR of the porous IOPCB in comparison with PCB, the IOPCB increases the density of the binding analyte molecules, and hence enlarges the detection concentration ranges of analytes. By merging IOPCB and core–shell SERS nanotags, the LDR was one order of magnitude higher than that of the PCB (Fig. 5d),[101] which is much larger than those of commercial ECLIA kits. Furthermore, multiplex analysis on a single IOPCB with encoded SERS nanotags was realized, although the LDR is decreased by one order of magnitude (10 pg mL^{-1}–10 μg mL^{-1} for AFP and CEA, Fig. 5e) due to the occupation of the surface area of the IOPCB by multiplex probes. In the multiplex assay, LODs of 3.6 and 1.9 fg mL^{-1} were obtained for AFP and CEA, respectively (Fig. 5e). This provides a new viewpoint for the development of the novel bioassay with large encoding capacity by position and spectrum encoding, as well as decreases the fabrication complexity and cost.

Summary and future directions

In this minireview, we outlined the basis of PhCs and plasmonics, and then highlighted the integration of PhCs and plasmonics for bioanalytical applications. By the hybridized photonic properties of PhC and plasmonic materials, novel biosensing substrates with ordered nanostructures will be designed and fabricated. The major advantages of the PhC–plasmonics hybrid sensors lie in four aspects: (1) *Enhanced detection sensitivity*: The spectral overlap of PhC and plasmonic resonance results in an enhanced light–material interaction, which in turn benefits detection sensitivity. (2) *Increased encoding capacity*: The multiplexed encoding strategy based on PhC reflection and the SERS spectrum can obviously increase encoding capacity, which is valuable for high throughput and multiplex detection. (3) *Enlarged surface area*: The inverse opal photonic crystal with a high surface to volume ratio provides high density analyte molecule binding sites, and hence enlarges the linear dynamic range. In addition, the nanostructured PhC backbone can effectively increase the density of plasmonic nanoparticles and produce stronger SERS signals. (4) *Multiplexed sensing modalities*: A sensor that can carry out different sensing mechanisms will be the tendency for the design of next-generation biosensors. Taking advantages of both PhC and plasmonic resonances, a hybrid device can be used as the transducer for refractive index, SERS, fluorescence, and photoacoustic measurements. Thus, the integration of PhCs and plasmonics opens the door to the design of a large variety of future analytical tools.

We expect more reliable power sensors to be fabricated in the future. Currently, hybrid sensors are still in their infancy, and some challenges need to be addressed. First, manufacturing costs need to be reduced. Recently, some nanoscale lithography methods, such as deep UV lithography, holographic lithography, and interference lithography, have significantly facilitated the fabrication of photonic crystal structures. However, new approaches, which are inexpensive and ready to scale up, are always desired for the preparation of mass PhC–plasmonic hybrid structures, especially in three dimensions. Second, detection throughput needs to be improved. Most of the proposed sensors can only detect one analyte at one time, resulting in low detection efficiency and increased detection time. Multiplex detection is urgently needed for clinical purposes and environmental monitoring in the big data era. Third, the sensitivity needs to be further increased to meet the demand of extremely low concentration analytes in the early period of some diseases. Nevertheless, we anticipate that the PhC–plasmonics hybrid sensor will draw increasing attention and more hybrid materials and techniques will emerge in the near future.

Conflicts of interest

There are no conflicts to declare.

Acknowledgements

This work was financially supported by the National Key Research and Development Program of China (No. 2017YFA0205700), the National Natural Science Foundation of China (Grants 21373046, 21327902, and 61675096), the Natural Science Foundation of Jiangsu Province (No. BK2014021828), the Fundamental Research Funds for the Central Universities, the Six Talent Peaks Project of Jiangsu Province, and the Collaboration Research Fund of Southeast University and Nanjing Medical University (Grant No. 2242017K3DN26). Meng Lu also thanks the support of the Antimicrobial Resistance Initiative (AMR) program at the Iowa State University, National Science Foundation (NSF), under grant ECCS 16-53673.

References

1 A. G. Brolo, *Nat. Photonics*, 2012, **6**, 709–713.
2 Y. Zhao, G. Chen, Y. Du, J. Xu, S. Wu, Y. Qu and Y. Zhu, *Nanoscale*, 2014, **6**, 13754–13760.
3 D. J. J. Hu and H. P. Ho, *Adv. Opt. Photonics*, 2017, **9**, 257–314.
4 H. Chen, R. Lou, Y. Chen, L. Chen, J. Lu and Q. Dong, *Drug Delivery*, 2017, **24**, 775–780.
5 Y. Leng, K. Sun, X. Chen and W. Li, *Chem. Soc. Rev.*, 2015, **44**, 5552–5595.
6 J. F. Li, Y. J. Zhang, S. Y. Ding, R. Panneerselvam and Z. Q. Tian, *Chem. Rev.*, 2017, **117**, 5002–5069.
7 F. Chiavaioli, F. Baldini, S. Tombelli, C. Trono and A. Giannetti, *Nanophotonics*, 2017, **6**, 663–679.
8 R. Gao, D. F. Lu, J. Cheng, Y. Jiang, L. Jiang, J. D. Xu and Z. M. Qi, *Biosens. Bioelectron.*, 2016, **86**, 321–329.
9 Y. C. Li, H. B. Xin, H. X. Lei, L. L. Liu, Y. Z. Li, Y. Zhang and B. J. Li, *Light: Sci. Appl.*, 2016, **5**, e16176.
10 E. Yablonovitch, *Phys. Rev. Lett.*, 1987, **58**, 2059–2062.
11 S. John, *Phys. Rev. Lett.*, 1987, **58**, 2486–2489.
12 B. Cunningham, B. Lin, J. Qiu, P. Li, J. Pepper and B. Hugh, *Sens. Actuators, B*, 2002, **85**, 219–226.
13 B. Cunningham, P. Li, B. Lin and J. Pepper, *Sens. Actuators, B*, 2002, **81**, 316–328.
14 B. T. Cunningham, P. Li, S. Schulz, B. Lin, C. Baird, J. Gerstenmaier, C. Genick, F. Wang, E. Fine and L. Laing, *J. Biomol. Screening*, 2004, **9**, 481–490.
15 Y. Tan, C. Ge, A. Chu, M. Lu, W. Goldshlag, C. S. Huang, A. Pokhriyal, S. George and B. T. Cunningham, *IEEE Sens. J.*, 2012, **12**, 1174–1180.
16 M. Lu, S. S. Choi, U. Irfan and B. T. Cunningham, *Appl. Phys. Lett.*, 2008, **93**, 481.
17 M. Lu, S. Choi, C. J. Wagner, J. G. Eden and B. T. Cunningham, *Appl. Phys. Lett.*, 2008, **92**, 219.
18 M. Minkov, V. Savona and D. Gerace, *Appl. Phys. Lett.*, 2017, **111**, 131104.
19 R. Gansch, S. Kalchmair, P. Genevet, T. Zederbauer, H. Detz, A. M. Andrews, W. Schrenk, F. Capasso, M. Loncar and G. Strasser, *Light: Sci. Appl.*, 2016, **5**, e16147.
20 K. E. Davis, W. B. Russel and W. J. Glantschnig, *Science*, 1989, **245**, 507–510.
21 T. C. Simonton, R. Roy, S. Komarneni and E. Breval, *J. Mater. Res.*, 1986, **1**, 667–674.
22 X. Chen, C. Chardin, K. Makles, C. Caer, S. Chua, R. Braive, I. Robert-Philip, T. Briant, P. F. Cohadon, A. Heidmann, T. Jacqmin and S. Deleglise, *Light: Sci. Appl.*, 2017, **6**, e16190.
23 Y. Tan, E. Sutanto, A. G. Alleyne and B. T. Cunningham, *J. Biophotonics*, 2014, **7**, 266–275.
24 E. Armstrong and C. O'Dwyer, *J. Mater. Chem. C*, 2015, **3**, 6109–6143.
25 A. E. Seago, P. Brady, J. P. Vigneron and T. D. Schultz, *J. R. Soc., Interface*, 2009, **6**, S165–S184.
26 M. Kolle and U. Steiner, *Encyclopedia of Nanotechnology*, 2012, pp. 2514–2527.
27 T. C. Garza, J. I. Scholtz, M. J. Gazes, I. Kymissis and N. K. Pervez, in *Next-Generation Spectroscopic Technologies Vii*, ed. M. A. Druy and R. A. Crocombe, 2014, p. 9101.
28 M. Nikoufard, M. Kazemi Alamouti and A. Adel, *Photonic Sens.*, 2016, **6**, 274–278.
29 K. Hwang, D. Kwak, C. Kang, D. Kim, Y. Ahn and Y. Kang, *Angew. Chem., Int. Ed.*, 2011, **50**, 6311–6314.
30 C. Zhu, L. Chen, H. Xu and Z. Gu, *Macromol. Rapid Commun.*, 2009, **30**, 1945–1949.
31 S. Tao, D. Chen, J. Wang, J. Qiao and Y. Duan, *Photonic Sens.*, 2016, **6**, 137–142.
32 M. F. H. Arif, K. Ahmed, S. Asaduzzaman and M. A. K. Azad, *Photonic Sens.*, 2016, **6**, 279–288.
33 S. Amrehn, X. Wu, C. Schumacher and T. Wagner, *Phys. Status Solidi A*, 2015, **212**, 1266–1272.
34 C. Fenzl, S. Wilhelm, T. Hirsch and O. S. Wolfbeis, *ACS Appl. Mater. Interfaces*, 2013, **5**, 173–178.
35 S. Aki, T. Endo, K. Sueyoshi and H. Hisamoto, *Anal. Chem.*, 2014, **86**, 11986–11991.
36 J. P. Couturier, M. Suetterlin, A. Laschewsky, C. Hettrich and E. Wischerhoff, *Angew. Chem., Int. Ed.*, 2015, **54**, 6641–6644.
37 Y. Zhao, H. Gu, Z. Xie, H. C. Shum, B. Wang and Z. Gu, *J. Am. Chem. Soc.*, 2013, **135**, 54–57.
38 Y. Zhao, Z. Xie, H. Gu, L. Jin, X. Zhao, B. Wang and Z. Gu, *NPG Asia Mater.*, 2012, **4**, e25.
39 L. Shang, F. Shangguan, Y. Cheng, J. Lu, Z. Xie, Y. Zhao and Z. Gu, *Nanoscale*, 2013, **5**, 9553–9557.
40 Z. Mu, X. Zhao, Y. Huang, M. Lu and Z. Gu, *Small*, 2015, **11**, 6036–6043.
41 A. Pokhriyal, M. Lu, C. Ge and B. T. Cunningham, *J. Biophotonics*, 2014, **7**, 332–340.

42 P. C. Mathias, H.-Y. Wu and B. T. Cunningham, *Appl. Phys. Lett.*, 2009, **95**, 21111.
43 W. Zhang, N. Ganesh, P. C. Mathias and B. T. Cunningham, *Small*, 2008, **4**, 2199–2203.
44 B. T. Cunningham and R. C. Zangar, *J. Biophotonics*, 2012, **5**, 617–628.
45 A. A. Yanik, A. E. Cetin, M. Huang, A. Artar, S. H. Mousavi, A. Khanikaev, J. H. Connor, G. Shvets and H. Altug, *Proc. Natl. Acad. Sci. U. S. A.*, 2011, **108**, 11784–11789.
46 B. Liu, S. Chen, J. Zhang, X. Yao, J. Zhong, H. Lin, T. Huang, Z. Yang, J. Zhu, S. Liu, C. Lienau, L. Wang and B. Ren, *Adv. Mater.*, 2018, **30**, 1706031.
47 J. F. Li, C.-Y. Li and R. F. Aroca, *Chem. Soc. Rev.*, 2017, **46**, 3962–3979.
48 C. Y. Chan, Z. L. Cao and H. C. Ong, *Opt. Express*, 2013, **21**, 14674–14682.
49 J. N. Anker, W. P. Hall, O. Lyandres, N. C. Shah, J. Zhao and R. P. Van Duyne, *Nat. Mater.*, 2008, **7**, 442–453.
50 L. B. Sagle, L. K. Ruvuna, J. A. Ruemmele and R. P. Van Duyne, *Nanomedicine*, 2011, **6**, 1447–1462.
51 P. L. Stiles, J. A. Dieringer, N. C. Shah and R. R. Van Duyne, *Annu. Rev. Anal. Chem.*, 2008, **1**, 601–626.
52 K. A. Willets and R. P. Van Duyne, *Annu. Rev. Phys. Chem.*, 2007, **58**, 267–297.
53 Y. Lan, S. Wang, X. Yin, Y. Liang, H. Dong, N. Gao, J. Li, H. Wang and G. Li, *Nanoscale*, 2016, **8**, 13454–13462.
54 D. Liu, C. Li, F. Zhou, T. Zhang, H. Zhang, X. Li, G. Duan, W. Cai and Y. Li, *Sci. Rep.*, 2015, **5**, 7686.
55 Z. Ma, L. Tian and H. Qiang, *J. Nanosci. Nanotechnol.*, 2009, **9**, 6716–6720.
56 G. Macias, M. Alba, L. F. Marsal and A. Mihi, *J. Mater. Chem. C*, 2016, **4**, 3970–3975.
57 A. Hessel and A. A. Oliner, *Appl. Opt.*, 1965, **4**, 1275–1297.
58 R. W. Day, S. S. Wang and R. Magnusson, *J. Lightwave Technol.*, 1996, **14**, 1815–1824.
59 S. S. Wang, R. Magnusson, J. S. Bagby and M. G. Moharam, *J. Opt. Soc. Am. A*, 1990, **7**, 1470–1474.
60 D. Wawro, S. Tibuleac, R. Magnusson and H. Liu, in *Biomedical Diagnostic, Guidance, and Surgical-Assist Systems Ii*, ed. T. VoDinh, W. S. Grundfest and D. A. Benaron, 2000, vol. 3911, pp. 86–94.
61 A. K. Kodali, M. Schulmerich, J. Ip, G. Yen, B. T. Cunningham and R. Bhargava, *Anal. Chem.*, 2010, **82**, 5697–5706.
62 J. N. Liu, M. V. Schulmerich, R. Bhargava and B. T. Cunningham, *Opt. Express*, 2014, **22**, 18142–18158.
63 A. Pokhriyal, M. Lu, V. Chaudhery, S. George and B. T. Cunningham, *Appl. Phys. Lett.*, 2013, **102**, 221114.
64 S. George, V. Chaudhery, M. Lu, M. Takagi, N. Amro, A. Pokhriyal, Y. Tan, P. Ferreira and B. T. Cunningham, *Lab Chip*, 2013, **13**, 4053–4064.
65 C. S. Huang, S. George, M. Lu, V. Chaudhery, R. Tan, R. C. Zangar and B. T. Cunningham, *Anal. Chem.*, 2011, **83**, 1425–1430.
66 A. Pokhriyal, M. Lu, V. Chaudhery, C. S. Huang, S. Schulz and B. T. Cunningham, *Opt. Express*, 2010, **18**, 24793–24808.
67 I. D. Block, N. Ganesh, M. Lu and B. T. Cunningham, *IEEE Sens. J.*, 2008, **8**, 274–280.
68 L. Liu, H. A. Khan, J. Li, A. C. Hillier and M. Lu, *Nanotechnology*, 2016, **27**, 295301.
69 M. Campbell, D. N. Sharp, M. T. Harrison, R. G. Denning and A. J. Turberfield, *Nature*, 2000, **404**, 53–56.
70 M. Miyake, Y.-C. Chen, P. V. Braun and P. Wiltzius, *Adv. Mater.*, 2009, **21**, 3012–3015.
71 W. Bogaerts, V. Wiaux, D. Taillaert, S. Beckx, B. Luyssaert, P. Bienstman and R. Baets, *IEEE J. Sel. Top. Quant.*, 2002, **8**, 928–934.
72 V. Chaudhery, S. George, M. Lu, A. Pokhriyal and B. T. Cunningham, *Sensors*, 2013, **13**, 5561–5584.
73 W. Zhang, N. Ganesh, I. D. Block and B. T. Cunningham, *Sens. Actuators, B*, 2008, **131**, 279–284.
74 S. M. Kim, W. Zhang and B. T. Cunningham, *Appl. Phys. Lett.*, 2008, **93**, 143112.
75 S. M. Kim, W. Zhang and B. T. Cunningham, *Opt. Express*, 2010, **18**, 4300–4309.
76 J. N. Liu, Q. Huang, K. K. Liu, S. Singamaneni and B. T. Cunningham, *Nano Lett.*, 2017, **17**, 7569–7577.
77 Y. F. Zhao, L. J. Liu, X. W. Zhao and M. Lu, *Appl. Phys. Lett.*, 2016, **109**, 835–2068.
78 Y. F. Zhao, K. Y. Liu, J. McClelland and M. Lu, *Appl. Phys. Lett.*, 2014, **104**, 89A–105A.
79 Y. Zhao, M. Cao, J. F. McClelland, Z. Shao and M. Lu, *Biosens. Bioelectron.*, 2016, **85**, 261–266.
80 Y. Zhao, Y. Huang, J. F. McClelland, X. Zhao and M. Lu, IEEE Photonics Conference, 2015.
81 Y. Zhao, L. Liu, X. Zhao and M. Lu, *Appl. Phys. Lett.*, 2016, **109**, 071108.
82 N. Narayanan, V. Karunakaran, W. Paul, K. Venugopal, K. Sujathan and K. K. Maiti, *Biosens. Bioelectron.*, 2015, **70**, 145–152.
83 H. N. Xie, R. Stevenson, N. Stone, A. Hernandez-Santana, K. Faulds and D. Graham, *Angew. Chem., Int. Ed.*, 2012, **51**, 8509–8511.
84 F. R. Madiyar, S. Bhana, L. Z. Swisher, C. T. Culbertson, X. Huang and J. Li, *Nanoscale*, 2015, **7**, 3726–3736.
85 J. Li, S. Dong, J. Tong, P. Zhu, G. Diao and Z. Yang, *Chem. Commun.*, 2016, **52**, 284–287.
86 J. U. Lee, A. H. Nguyen and S. J. Sim, *Biosens. Bioelectron.*, 2015, **74**, 341–346.
87 D. K. Lim, K. S. Jeon, J. H. Hwang, H. Kim, S. Kwon, Y. D. Suh and J. M. Nam, *Nat. Nanotechnol.*, 2011, **6**, 452–460.
88 S. Y. Ding, J. Yi, J. F. Li, B. Ren, D. Y. Wu, R. Panneerselvam and Z. Q. Tian, *Nat. Rev. Mater.*, 2016, **1**, 16021.
89 J. Hou, H. Zhang, Q. Yang, M. Li, Y. Song and L. Jiang, *Angew. Chem., Int. Ed.*, 2014, **53**, 5791–5795.
90 B. Bao, M. Li, Y. Li, J. Jiang, Z. Gu, X. Zhang, L. Jiang and Y. Song, *Small*, 2015, **11**, 1649–1654.
91 Y. Li, Q. Yang, M. Li and Y. Song, *Sci. Rep.*, 2016, **6**, 24628.

92 X. Zhao, J. Xue, Z. Mu, Y. Huang, M. Lu and Z. Gu, *Biosens. Bioelectron.*, 2015, **72**, 268–274.
93 D. Wang, X. Zhao, X. Liu, Z. Mu and Z. Gu, *Nano Res.*, 2016, **9**, 2760–2771.
94 X. Zhao, Y. Zhao and Z. Gu, *Sci. China: Chem.*, 2011, **54**, 1185–1201.
95 B. Liu, X. Zhao, W. Jiang, D. Fu and Z. Gu, *Nanoscale*, 2016, **8**, 17465–17471.
96 K. C. Bantz, A. F. Meyer, N. J. Wittenberg, H. Im, O. Kurtulus, S. H. Lee, N. C. Lindquist, S. H. Oh and C. L. Haynes, *Phys. Chem. Chem. Phys.*, 2011, **13**, 11551–11567.
97 B. Liu, H. Ni, D. Zhang, D. Wang, D. Fu, H. Chen, Z. Gu and X. Zhao, *ACS Sens.*, 2017, **2**, 1035–1043.
98 J. B. Lassiter, J. Aizpurua, L. I. Hernandez, D. W. Brandl, I. Romero, S. Lal, J. H. Hafner, P. Nordlander and N. J. Halas, *Nano Lett.*, 2008, **8**, 1212–1218.
99 L. Lin, H. Gu and J. Ye, *Chem. Commun.*, 2015, **51**, 17740–17743.
100 E. Prodan, C. Radloff, N. J. Halas and P. Nordlander, *Science*, 2003, **302**, 419–422.
101 B. Liu, D. Zhang, H. Ni, D. Wang, L. Jiang, D. Fu, X. Han, C. Zhang, H. Chen, Z. Gu and X. Zhao, *ACS Appl. Mater. Interfaces*, 2018, **10**, 21–26.